

THERMOELECTRICAL PROPERTIES OF A MONOCRYSTALLINE $\text{Al}_{64}\text{Cu}_{23}\text{Fe}_{13}$ QUASICRYSTAL

TERMOELEKTRIČNE LASTNOSTI MONOKRISTALNEGA KVAZIKRISTALA $\text{Al}_{64}\text{Cu}_{23}\text{Fe}_{13}$

Igor Smiljanić¹, Ante Bilušić^{1,2}, Željko Bihar¹, Jagoda Lukatela¹, Boran Leontić¹,
Janez Dolinšek³, Ana Smontara¹

¹Institute of Physics, Bijenička 46, HR-10000 Zagreb, Croatia

²Faculty of Natural Sciences, University of Split, N. Tesle 12, HR-21000 Split, Croatia

³J. Stefan Institute, Jamova 39, SI-1000 Ljubljana, Slovenia
ismiljanic@ifs.hr

Prejem rokopisa – received: 2007-07-12; sprejem za objavo – accepted for publication: 2007-08-01

We performed investigations of the electrical resistivity, thermopower and thermal conductivity of a monocrystalline $i\text{-Al}_{64}\text{Cu}_{23}\text{Fe}_{13}$ as well as a polycrystalline $i\text{-Al}_{63}\text{Cu}_{25}\text{Fe}_{12}$ icosahedral quasicrystal, for comparison. The electrical resistivity of both samples, the monocrystalline $i\text{-Al}_{64}\text{Cu}_{23}\text{Fe}_{13}$ and the polycrystalline $i\text{-Al}_{63}\text{Cu}_{25}\text{Fe}_{12}$, exhibits a negative temperature coefficient with $\rho_{4\text{K}} = 3950 \mu\Omega \text{ cm}$ and $\rho_{4\text{K}} = 4900 \mu\Omega \text{ cm}$, and the ratio $\rho_{4\text{K}}/\rho_{300\text{K}} = 1.8$, $\rho_{4\text{K}}/\rho_{300\text{K}} = 1.7$, respectively. The thermopowers are large and have a negative sign. In addition, the thermopower of the monocrystalline $i\text{-Al}_{64}\text{Cu}_{23}\text{Fe}_{13}$ exhibits a sign reversal at $T = 278 \text{ K}$. The thermal conductivity is anomalously low, of the order of 1 W/mK at room temperature, with a slightly different temperature variation at low temperatures. On the basis of these results, we concluded that there are no systematic differences between the high-quality monocrystalline and polycrystalline icosahedral $i\text{-Al-Cu-Fe}$ quasicrystals. Moreover, the reported transport properties of $i\text{-Al-Cu-Fe}$ appear to be intrinsic to this family of icosahedral quasicrystals.

Keywords: quasicrystals; $i\text{-AlCuFe}$, physical properties, resistivity, thermal conductivity

Raziskali smo električno prevodnost, termonapetost in toplotno prevodnost monokristalnega $i\text{-Al}_{64}\text{Cu}_{23}\text{Fe}_{13}$ in za primerjavo tudi polikristalnega ikozaedričnega kvazikristala $i\text{-Al}_{63}\text{Cu}_{25}\text{Fe}_{12}$. Električna upornost obeh vzorcev ima negativen temperaturni koeficient z $\rho_{4\text{K}} = 3950 \mu\Omega \text{ cm}$ in $\rho_{4\text{K}} = 4900 \mu\Omega \text{ cm}$, ter razmerje $\rho_{4\text{K}}/\rho_{300\text{K}} = 1.8$, $\rho_{4\text{K}}/\rho_{300\text{K}} = 1.7$. Termonapetosti so velike in z negativnim predznakom, termonapetost monokristalnega $i\text{-Al}_{64}\text{Cu}_{23}\text{Fe}_{13}$ pa ima spremembo predznaka pri $T = 278 \text{ K}$. Toplotna prevodnost je anormalno majhna, je reda velikosti 1 W/mK pri sobni temperaturi in z nekoliko drugačno temperaturno odvisnostjo pri nizki temperaturi. Na podlagi rezultatov meritev sklepamo, da ni sistematične razlike med visokokakovostnima monokristalnima in mnogokristalnima ikozaedričnima kvazikristaloma $i\text{-Al-Cu-Fe}$. Poleg tega so transportne lastnosti $i\text{-Al-Cu-Fe}$ značilne za to družino ikozaedričnih kvazikristalov.

Ključne besede: kvazikristali, $i\text{-AlCuFe}$, fizikalne lastnosti, upornost, toplotna prevodnost

1 INTRODUCTION

The family of icosahedral $i\text{-Al-Cu-Fe}$ quasicrystals is currently one of the most studied, due to its excellent thermal stability. Most studies reported so far were performed on polycrystalline samples, and include investigations of the electrical resistivity and magnetoresistance,¹⁻⁹ thermoelectric power,⁹⁻¹² thermal conductivity,^{2,9,13} magnetism,^{3,8,14} and Hall coefficient.^{1,5,7,8} Though polycrystalline samples may acquire quite a high structural perfection through a proper thermal annealing procedure, rapid quenching to room temperature after annealing inevitably results in a strained material that also contains high thermal vacancy concentration for the room temperature conditions (i.e., the quenched-in vacancy concentration is in equilibrium for the much higher temperature of annealing). In addition, grain boundaries may hinder the propagation of electrons and phonons, thus affecting long-range electrical and heat-transport phenomena. In order to test for the true intrinsic properties of $i\text{-Al-Cu-Fe}$ quasicrystals, it is desirable to compare the physical properties of the polycrystalline material with those measured on

high-quality monocrystalline samples, where structural imperfections are largely absent. Therefore, we have performed a study by investigating the electrical resistivity, the thermoelectric power and the thermal conductivity of a monocrystalline $i\text{-Al}_{64}\text{Cu}_{23}\text{Fe}_{13}$ and a polycrystalline $i\text{-Al}_{63}\text{Cu}_{25}\text{Fe}_{12}$ quasicrystal.

2 EXPERIMENTAL PROCEDURE

We investigated two samples with slightly different compositions, a monocrystalline $i\text{-Al}_{64}\text{Cu}_{23}\text{Fe}_{13}$ (in the following text abbreviated as $i\text{-Al}_{64}\text{Cu}_{23}\text{Fe}_{13}$) and a polycrystalline $i\text{-Al}_{63}\text{Cu}_{25}\text{Fe}_{12}$ icosahedral quasicrystal (in the following text abbreviated as $i\text{-Al}_{63}\text{Cu}_{25}\text{Fe}_{12}$). The $i\text{-Al}_{63}\text{Cu}_{25}\text{Fe}_{12}$ were made from large polycrystalline ingots prepared by conventional casting and subsequent annealing, and it was verified with X-ray diffraction that the samples are single-phase icosahedral. A large monocrystalline $i\text{-Al}_{64}\text{Cu}_{23}\text{Fe}_{13}$ quasicrystal was prepared by the Czochralski technique and annealing removed the strains. It has an almost phason-free quasicrystalline structure and shows superior quasicrystallinity on both the macro- and microscopic scales. The samples were

shaped in the form of a prism, with dimensions $3.9 \text{ mm} \times 1.5 \text{ mm} \times 1.4 \text{ mm}$ ($i\text{-Al}_{64}\text{Cu}_{23}\text{Fe}_{13}$) and $7.2 \text{ mm} \times 1.6 \text{ mm} \times 1.2 \text{ mm}$ ($i\text{-Al}_{63}\text{Cu}_{25}\text{Fe}_{12}$). The electrical resistivity was measured by a standard four-probe technique with applied currents of 0.1 mA to 1 mA, while the thermoelectric power was measured with respect to high-purity gold lead wires, using a deferential technique. The thermal conductivity was measured using an absolute steady-state heat-flow method. The thermal flux was generated by a 1 k Ω RuO₂ chip-resistor glued to one end of the sample, while the other end was attached to a copper heat sink. The temperature gradient across the sample was monitored by a chromel-constantan differential thermocouple.

3 RESULTS AND ANALYSIS

3.1 Electrical resistivity and thermopower

The electrical resistivity ($\rho(T)$) and thermopower ($S(T)$) of $i\text{-Al}_{64}\text{Cu}_{23}\text{Fe}_{13}$ and $i\text{-Al}_{63}\text{Cu}_{25}\text{Fe}_{12}$ were measured in the temperature range from 4 K to 300 K. The results are shown in **Figure 1** and **Figure 2**. The resistivities of $i\text{-Al}_{64}\text{Cu}_{23}\text{Fe}_{13}$ and $i\text{-Al}_{63}\text{Cu}_{25}\text{Fe}_{12}$ exhibit a negative temperature coefficient, the room temperature values are $\rho_{300\text{K}} = 2200 \text{ }\mu\Omega \text{ cm}$ and $\rho_{300\text{K}} = 2900 \text{ }\mu\Omega \text{ cm}$ respectively and the total increases of resistivity is by factors of $R = \rho_{4\text{K}}/\rho_{300\text{K}} = 1.8$ and $R = \rho_{4\text{K}}/\rho_{300\text{K}} = 1.7$, respectively. In addition, $\rho(T)$ of the $i\text{-Al}_{64}\text{Cu}_{23}\text{Fe}_{13}$ exhibits a weakly pronounced maximum with the peak value $\rho_{300\text{K}} = 4040 \text{ }\mu\Omega \text{ cm}$, at 20 K. The thermopowers $S(T)$ are, in general, large and, in addition, exhibit an interesting feature of a sign reversal (**Figure 2**) in the case of $i\text{-Al}_{64}\text{Cu}_{23}\text{Fe}_{13}$. Below 120 K, $S(T)$ is negative with a negative slope, whereas around 120 K it exhibits a minimum and the slope is reversed. Consequently, the

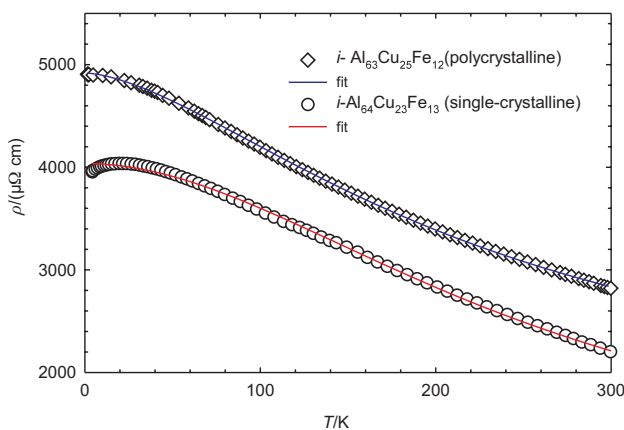


Figure 1: Electrical resistivity of the polycrystalline $i\text{-Al}_{63}\text{Cu}_{25}\text{Fe}_{12}$ and monocrystalline $i\text{-Al}_{64}\text{Cu}_{23}\text{Fe}_{13}$, respectively. The fits (solid lines) of $\rho(T)$ and $S(T)$ were made simultaneously with the Kubo-Greenwood formalism using the spectral resistivity function $\rho(\epsilon)$.

Slika 1: Električna upornost polikristalnega $i\text{-Al}_{63}\text{Cu}_{25}\text{Fe}_{12}$ in monokristalnega $i\text{-Al}_{64}\text{Cu}_{23}\text{Fe}_{13}$. Približek (cele črte) $\rho(T)$ in $S(T)$ je napravljen istočasno s Kubo-Greenwood formalizmom z uporabo funkcije spektralne upornosti $\rho(\epsilon)$

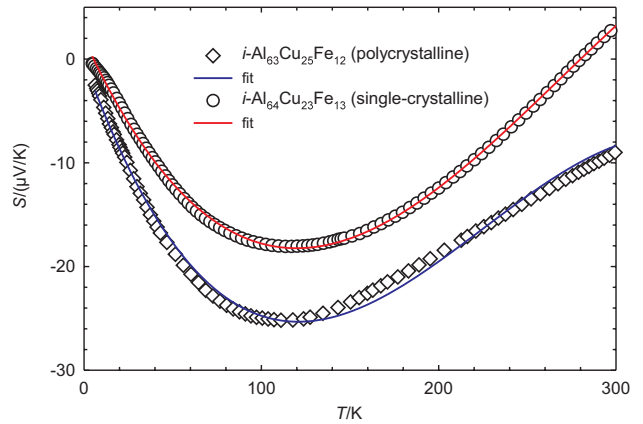


Figure 2: Thermopower of the monocrystalline $i\text{-Al}_{64}\text{Cu}_{23}\text{Fe}_{13}$ and the polycrystalline $i\text{-Al}_{63}\text{Cu}_{25}\text{Fe}_{12}$, respectively. The fits (solid lines) of $\rho(T)$ and $S(T)$ were made simultaneously with the Kubo-Greenwood formalism using the spectral resistivity function $\rho(\epsilon)$.

Slika 2: Termoponetost monokristalnega $i\text{-Al}_{64}\text{Cu}_{23}\text{Fe}_{13}$ in polikristalnega $i\text{-Al}_{63}\text{Cu}_{25}\text{Fe}_{12}$. Približek (cele črte) za $\rho(T)$ in $S(T)$ je pripravljen istočasno s Kubo-Greenwood formalizmom in z uporabo funkcije spektralne upornosti $\rho(\epsilon)$

$S(T)$ of $i\text{-Al}_{64}\text{Cu}_{23}\text{Fe}_{13}$ changes sign to positive at $T = 278 \text{ K}$.

For the analysis of $\rho(T)$ and $S(T)$ we used the spectral resistivity model of Landau and Solbrig,^{11,12,16} where both quantities are analyzed simultaneously by presuming a specific structure- and composition-related form of the energy-dependent spectral resistivity function $\rho(\epsilon)$ (or its inverse, the spectral conductivity $\sigma(\epsilon) = 1/\rho(\epsilon)$). Using the Kubo-Greenwood formalism, the temperature-dependent electrical conductivity is calculated according to

$$\sigma(T) = \int d\epsilon \sigma(\epsilon) \left(-\frac{\partial f(\epsilon, T)}{\partial \epsilon} \right) \quad (1)$$

whereas the thermopower is obtained from

$$S(T) = -\frac{k_B}{|e|\sigma(T)} \int d\epsilon \sigma(\epsilon) \left(\frac{\epsilon - \mu(T)}{k_B T} \right) \left(-\frac{\partial f(\epsilon, T)}{\partial \epsilon} \right) \quad (2)$$

Here, $f(\epsilon, T) = \{\exp[(\epsilon - \mu)/k_B T] + 1\}^{-1}$ is the Fermi-Dirac function and $\mu(T)$ is the chemical potential, which is written in the low-temperature representation as¹⁷

$$\mu(T) = \epsilon_F - (k_B T)^2 \frac{\pi^2}{6} \left(\frac{d \ln n(\epsilon)}{d\epsilon} \right)_{\epsilon_F} = \epsilon_F - \xi T^2 \quad (3)$$

The electronic density of states $n(\epsilon)$ is related to the spectral conductivity via the Einstein relation $\sigma(\epsilon) = (e^2/V)n(\epsilon)D(\epsilon)$ with $D(\epsilon)$ being the electronic spectral diffusivity. The only material-dependent quantity in Eqs. (1–3) is $\sigma(\epsilon)$, so that a proper model of the spectral conductivity should reproduce both $\sigma(T)$ and $S(T)$ at the same time.

The *ab-initio*-derived spectral resistivity could be modeled by the superposition of two Lorentzians

$$\rho(\varepsilon) = A \left\{ \left[\frac{1}{\pi} \frac{\gamma_1}{(\varepsilon - \delta_1)^2 + \gamma_1^2} \right] + \alpha \left[\frac{1}{\pi} \frac{\gamma_2}{(\varepsilon - \delta_2)^2 + \gamma_2^2} \right] \right\} \quad (4)$$

where $1/\pi\gamma_i$ is the height of a Lorentzian, $2\gamma_i$ its FWHM, δ_i its position with respect to the Fermi energy ε_F (taken to be at the origin of the energy scale; $\varepsilon_F = 0$) and α is the relative weight of the Lorentzians. The position of the narrow resistivity peak with respect to the Fermi energy ε_F is responsible for the anomalous electronic transport properties. As this peak is due to a specific distribution of Fe atoms in the structure, quasiperiodicity alone cannot account for the anomalous transport properties of *i*-Al-Cu-Fe quasicrystals; a right chemical decoration is also needed. The Fermi energy can be shifted on the scale of a few 100 meV by deviations in the stoichiometry and/or by defects in both structure and chemical decoration,^{18,19} so that the relative position of the narrow peak can change on this energy scale in samples of slightly different composition and annealing treatment. Consequently, solely on the basis of small shifts of ε_F , the thermopower of *i*-Al-Cu-Fe samples of similar composition can switch between large positive and large negative values and it may also change sign with temperature, as demonstrated for the *i*-Al₆₂Cu_{25.5}Fe_{12.5} polycrystalline sample.^{9,10,12} The fits of the experimental $\rho(T)$ and $S(T)$ data were performed simultaneously with Eqs. (1-4) by adjusting the set of parameters (A , α , δ_1 , δ_2 , γ_1 and γ_2) pertinent to the shape of the spectral resistivity $\rho(\varepsilon)$. The starting value of the parameter ξ entering the temperature-dependent chemical potential of Eq. (3) was determined by recognizing that in the case when the spectral variation of the electronic diffusivity can be neglected, one can replace $n(\varepsilon)$ by $\sigma(\varepsilon)$ in Eq. (3). The initial value was obtained by using the Mott formula

$$S^{\text{Mott}}(T) = \frac{\pi^2}{3} \frac{k_B^2}{|e|} \left(\frac{d \ln \sigma(\varepsilon)}{d\varepsilon} \right)_{\varepsilon_F} T$$

so that $\xi = -0.5|e|(S^{\text{Mott}}(T)/T)$. The fits are shown as solid lines in **Figure 1** and **Figure 2**; the fit parameters are

collected in **Table 1**. The fits of both $\rho(T)$ and $S(T)$ are excellent in the whole investigated temperature range.

The magnitude of the electrical resistivity of the monocrystalline *i*-Al₆₄Cu₂₃Fe₁₃ is in-line with the values reported for the polycrystalline *i*-Al-Cu-Fe. In polycrystalline *i*-Al-Cu-Fe the total variation of $\rho(T)$ over the relevant Fe range is merely a factor of two,⁵ so that the material is best classified as a semi-metal over the whole icosahedral concentration range with no indication of a large resonant increase of the resistivity. The ρ_{4K} resistivity value of our *i*-Al₆₄Cu₂₃Fe₁₃ matches well with that of the polycrystalline samples from the study⁵ with the same Fe concentration. However, since the Fermi energy of our *i*-Al₆₄Cu₂₃Fe₁₃ is located nearly at the maximum of the spectral resistivity²⁰, further shifts of ε_F over the resistivity peak due to a small variation of the Fe composition would not result in an additional increase of the resistivity, but can only make it smaller. This hints that the factor-of-two larger peak resistivity of the polycrystalline *i*-Al-Cu-Fe material at the Fe 12.5 % concentration,⁵ as compared to the monocrystalline *i*-Al₆₄Cu₂₃Fe₁₃, could originate in extrinsic factors like grain boundaries and other lattice imperfections that act as additional scattering centers for the conduction electrons.

3.2 Thermal conductivity

The measured thermal conductivities $\kappa(T)$ of *i*-Al₆₄Cu₂₃Fe₁₃ and *i*-Al₆₃Cu₂₅Fe₁₂ are displayed in **Figure 3**. The conductivity value at room temperature of *i*-Al₆₄Cu₂₃Fe₁₃ amounts $\kappa_{300K} = 1.7 \text{ W/mK}$, whereas in the case of the *i*-Al₆₃Cu₂₅Fe₁₂ is $\kappa_{300K} = 2.9 \text{ W/mK}$. These values are surprisingly low for an alloy of regular metals and are comparable to the thermal conductivities of known thermal insulators, amorphous fused silica²¹ and the technologically widespread thermally insulating material, yttrium-doped zirconia ceramics²². The $\kappa(T)$ data were analyzed with a semi-quantitative model, appropriate for icosahedral quasicrystals and their approximants²²⁻²⁹. The thermal conductivity parameter $\kappa(T)$ is divided into three terms

Table 1: Parameters of the spectral resistivity $\rho(\varepsilon)$ of Eq. (4), obtained from the simultaneous fits of $\rho(T)$ and $S(T)$ for *i*-Al₆₄Cu₂₃Fe₁₃ (monocrystalline) and *i*-Al₆₃Cu₂₅Fe₁₂ (polycrystalline)

Tabela 1: Parameter posebne upornosti $\rho(\varepsilon)$ enačba (4), določen z istočasnim približkom $\rho(T)$ in $S(T)$ za *i*-Al₆₄Cu₂₃Fe₁₃ (monokristalen) in *i*-Al₆₃Cu₂₅Fe₁₂ (polikristalen)

sample Al-Cu-Fe	$A/(\mu\Omega \text{ cm eV})$	$d_1/(\text{meV})$	$\gamma_1/(\text{meV})$	α	$d_2/(\text{meV})$	$\gamma_2/(\text{meV})$
mono-crystalline	392	-43	241	1.13	-9	38
polycrystalline	847	-5.2	587	1.07	-16	55

Table 2: Fit parameters of the thermal conductivity $\kappa(T)$ *i*-Al₆₄Cu₂₃Fe₁₃ (monocrystalline) and *i*-Al₆₃Cu₂₅Fe₁₂ (polycrystalline), respectively

Tabela 2: Parametri približka toplotne prevodnosti $\kappa(T)$ za *i*-Al₆₄Cu₂₃Fe₁₃ (monokristalen) in *i*-Al₆₃Cu₂₅Fe₁₂ (polikristalen)

sample Al-Cu-Fe	L_{eff}	$\kappa_H^0(\text{W/mK})$	$E_a/(\text{meV})$	$A/(\text{s}^{-1}\text{K}^{-2})$	$B/(\text{s}^{-1}\text{K}^{-4})$	β
mono-crystalline	2.1	0.7	6.3	1.2×10^7	2.8×10^4	3.2
polycrystalline	2.5	2.2	16.2	3.5×10^6	7.2×10^3	2.0

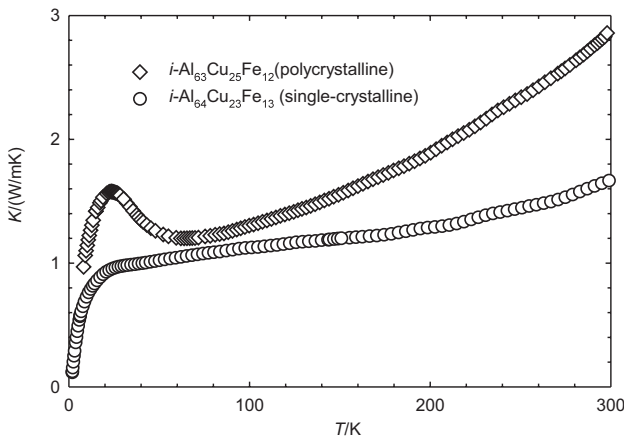


Figure 3: Thermal conductivity $\kappa(T)$ of the monocrystalline $i\text{-Al}_{64}\text{Cu}_{23}\text{Fe}_{13}$ and the polycrystalline $i\text{-Al}_{63}\text{Cu}_{25}\text{Fe}_{12}$, respectively
Slika 3: Toplotna prevodnost $\kappa(T)$ za monokristalni $i\text{-Al}_{64}\text{Cu}_{23}\text{Fe}_{13}$ in polikristalni $i\text{-Al}_{63}\text{Cu}_{25}\text{Fe}_{12}$

$$\kappa(T) = \kappa_{\text{el}}(T) + \kappa_{\text{D}}(T) + \kappa_{\text{H}}(T) \quad (5)$$

The electronic contribution κ_{e} is obtained using the empirical Wiedemann-Franz law ($\kappa_{\text{el}} = L_0 \sigma T$) with a temperature-dependent effective Lorenz number

$$L(T) = \frac{\kappa_{\text{el}}(T)}{T \times \sigma(T)} \quad (6)$$

The lattice contribution ($\kappa - \kappa_{\text{el}}$) is analyzed by considering (i) the propagation of long-wavelength acoustic phonons (for which the quasicrystal structure is an elastic continuum) within the Debye model and (ii) hopping of localized vibrations within the icosahedral cluster substructure, which participate in the heat transfer via thermally activated hopping. In the simplest model, the hopping of localized vibrations is described by a single activation energy E_{a} , yielding a contribution to the thermal conductivity

$$\kappa_{\text{H}} = \kappa_{\text{H}}^0 \exp\left(\frac{-E_{\text{a}}}{k_{\text{B}} T}\right) \quad (7)$$

where κ_{H}^0 is a constant. The Debye thermal conductivity is written as³⁰

$$\kappa_{\text{D}} = C_{\text{D}} T^3 \int_0^{\theta_{\text{D}}/T} \tau(x) \frac{x^4 e^x}{(e^x - 1)^2} dx \quad (8)$$

where $C_{\text{D}} = k_{\text{B}}^4 / 2\pi^2 \bar{v} \hbar^3$, \bar{v} is the average sound velocity, θ_{D} the Debye temperature, τ the phonon relaxation time and $x = \hbar\omega / k_{\text{B}} T$, where $\hbar\omega$ is the phonon energy. The different phonon-scattering processes are incorporated into the relaxation time $\tau(x)$ and we assume that Matthiessen's rule is valid, $\tau^{-1} = \sum \tau_j^{-1}$, where τ_j^{-1} is the scattering rate related to the j -th scattering channel. In analogy with the Al-Pd-Mn approximant and quasicrystal phases,^{24,25,30} we consider two dominant scattering processes in the investigated temperature range: (1) the scattering of phonons on structural defects of stacking-fault type with the

scattering rate $\tau_{\text{sf}}^{-1} = A x^2 T^2$ and (2) *umklapp* processes with the phenomenological form of the scattering rate pertinent to quasicrystals,^{23,24,29} $\tau_{\text{um}}^{-1} = B x^{\beta} T^{4-\beta}$, so that $\tau^{-1} = \tau_{\text{sf}}^{-1} + \tau_{\text{um}}^{-1}$. The Debye temperature of $i\text{-Al-Cu-Fe}$ was estimated from the specific heat³² as $\theta_{\text{D}} \approx 560$ K and the Debye constant C_{D} was determined from ultrasonic data³⁰. The fits (solid lines in **Figure 4**) are excellent and the fit parameters are collected in **Table 2**. The electronic (κ_{el}), Debye (κ_{D}) and hopping (κ_{H}) contributions are shown separately on the graph. The temperature-dependent effective Lorenz number $L(T)$ of $i\text{-Al}_{64}\text{Cu}_{23}\text{Fe}_{13}$ and $i\text{-Al}_{63}\text{Cu}_{25}\text{Fe}_{12}$ deviates considerably from the Wiedemann-Franz value L_0 , amounting $L/L_0 = 2.1$ and $L/L_0 = 2.5$ at 300 K, respectively, and the electrons carry around 40 % of the total heat in both cases. The Debye contribution exhibits a maximum at about 30 K and declines above this temperature, whereas the hopping contribution becomes significant at elevated temperatures. The activation energy for the hopping of $i\text{-Al}_{64}\text{Cu}_{23}\text{Fe}_{13}$ and $i\text{-Al}_{63}\text{Cu}_{25}\text{Fe}_{12}$ was determined as $E_{\text{a}} \approx 16$ meV and $E_{\text{a}} \approx 16$ meV, respectively. These energies correlate with the inelastic neutron and X-ray scattering experiments on $i\text{-Al-Pd-Mn}$ quasicrystals, where dispersionless vibrational states were identified for energies higher than 12 meV. Such dispersionless states indicate localized vibrations and are considered to be a consequence of a dense distribution of energy gaps in the phonon excitation spectrum of quasicrystals. The parameters B and β define phonon scattering by *umklapp* processes in a phenomenological way. The fit-determined $\beta = 3.2$ value for $i\text{-Al}_{64}\text{Cu}_{23}\text{Fe}_{13}$ yields

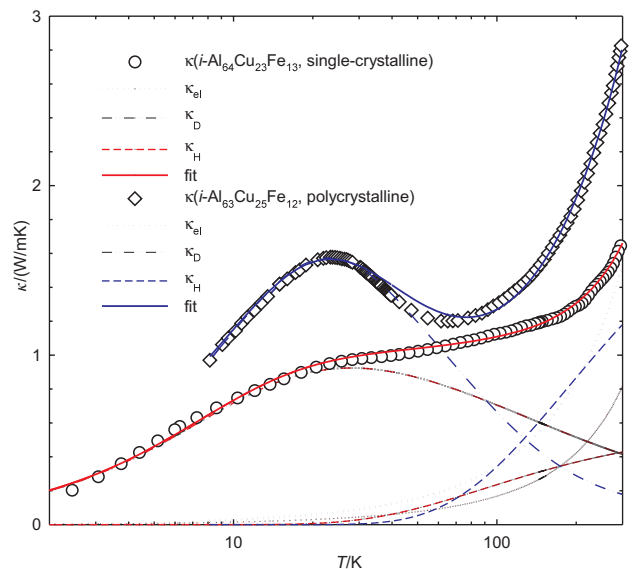


Figure 4: Thermal conductivity $\kappa(T)$ with the fits to the total $\kappa(T)$, of the monocrystalline $i\text{-Al}_{64}\text{Cu}_{23}\text{Fe}_{13}$ and the polycrystalline $i\text{-Al}_{63}\text{Cu}_{25}\text{Fe}_{12}$. The three contributions to the total $\kappa(T)$, electronic κ_{el} , Debye κ_{D} and hopping κ_{H} , are shown separately

Slika 4: Toplotna prevodnost $\kappa(T)$ s približkom za skupen $\kappa(T)$, za monokristalni $i\text{-Al}_{64}\text{Cu}_{23}\text{Fe}_{13}$ in za polikristalni $i\text{-Al}_{63}\text{Cu}_{25}\text{Fe}_{12}$. Posebej so prikazani trije prispevki k skupni $\kappa(T)$, elektronski κ_{el} , Debye κ_{D} in preskočna κ_{H}

the frequency- and temperature dependence of the *umklapp* term $\tau_{\text{um}}^{-1} \propto \omega^{3.2} T^{0.8}$ and indicates similarity with the modified quasi-umklapp scattering rate $\tau_{\text{um}}^{-1} \propto \omega^3 T$, used for the analysis of the thermal conductivity of *i*-Zn-Mg-Y quasicrystals, while for the polycrystalline sample, the fit-determined $\beta = 2.0$ $\tau_{\text{um}}^{-1} \propto \omega^2 T^2$ indicates the quasi-umklapp scattering rate obtained for the *i*-Al-Pd-Mn quasicrystals^{25,29}. Here it should be mentioned that the Debye and hopping contributions slightly compensate for each other in the fit procedure, so that the parameter values characterizing κ_{D} and κ_{H} should be considered at the qualitative level.

Regarding the comparison of the thermal conductivity of monocrystalline and polycrystalline *i*-Al-Cu-Fe, we are not aware of other quantitative analyses of $\kappa(T)$ of polycrystalline samples in the sense of Eqs. (5–8), so that the comparison has to be made at the level of experimental thermal conductivities. The room-temperature value for *i*- $\text{Al}_{64}\text{Cu}_{23}\text{Fe}_{13}$ amounts to $\kappa_{300\text{K}} = 1.7$ W/mK, whereas for the *i*- $\text{Al}_{63}\text{Cu}_{25}\text{Fe}_{12}$ it is $\kappa_{300\text{K}} = 2.9$ W/mK. Though the scatter of the known values of thermal conductivity of *i*-Al-Cu-Fe³⁴ is relatively large, there seems to be no systematic difference between the polycrystalline and monocrystalline samples.

4 CONCLUSION

We performed investigations of electrical resistivity, thermoelectric power and thermal conductivity on a monocrystalline *i*- $\text{Al}_{64}\text{Cu}_{23}\text{Fe}_{13}$ and a polycrystalline *i*- $\text{Al}_{63}\text{Cu}_{25}\text{Fe}_{12}$ icosahedral quasicrystal, for comparison. The electrical resistivity and thermopower analysis shows that the Fermi energy is located at the minimum of the pseudogap in the spectral conductivity $\sigma(\varepsilon)$. All this gives evidence that we are dealing with icosahedral quasicrystal samples of exceptional quality, so that its physical properties may be considered as intrinsic to the *i*-Al-Cu-Fe phase. A comparison of the investigated monocrystalline *i*- $\text{Al}_{64}\text{Cu}_{23}\text{Fe}_{13}$ to the polycrystalline *i*- $\text{Al}_{63}\text{Cu}_{25}\text{Fe}_{12}$, however, shows that there are no pronounced differences between the two forms of the material. While there are essentially no differences in the magnetic properties of the monocrystalline and polycrystalline materials, the electrical resistivity of the polycrystalline material is larger by a factor of two. This difference can be easily accounted for by the grain boundaries and other lattice imperfections that act as additional scattering centers for the conduction electrons. Comparing the thermopowers of the monocrystalline and polycrystalline *i*-Al-Cu-Fe materials, in general, the $S(T)$ magnitude and temperature dependence depend strongly on the position of ε_{F} relative to the spectral resistivity peak, so that slight differences in the samples' stoichiometry and structural perfection may lead to very different thermopowers in both magnitude and sign. A

quantitative comparison of the thermal conductivities of monocrystalline and polycrystalline *i*-Al-Cu-Fe is less straightforward due to the random scatter of the reported values, but $\kappa_{300\text{K}}$ of the monocrystalline *i*- $\text{Al}_{64}\text{Cu}_{23}\text{Fe}_{13}$ fits within the range of values for the polycrystalline *i*- $\text{Al}_{63}\text{Cu}_{25}\text{Fe}_{12}$. To conclude, we found no systematic differences in the electrical resistivity, thermoelectric power and thermal conductivity between the high-quality monocrystalline and polycrystalline *i*-Al-Cu-Fe quasicrystals, and the reported physical properties of the other *i*-Al-Cu-Fe quasicrystals appear to be intrinsic to this family of icosahedral quasicrystals.

Acknowledgements

We would like to thank Y. Yokoyama and Y. Calvayrac for giving us the samples of monocrystalline *i*- $\text{Al}_{64}\text{Cu}_{23}\text{Fe}_{13}$ and polycrystalline *i*- $\text{Al}_{63}\text{Cu}_{25}\text{Fe}_{12}$ icosahedral quasicrystal, respectively. This work was done within the activities of the 6th Framework EU Network of Excellence "Complex Metallic Alloys" (Contract No. NMP3-CT-2005-500140), and has been supported in part by the Ministry of Science, Education and Sports of Republic of Croatia through the Research Projects Nos. 035-0352826-2848 and 177-0352828-0478.

5 REFERENCES

- 1 T. Klein, A. Gozlan, C. Berger, F. Cyrot-Lackmann, Y. Calvayrac, A. Quivy, Europhys. Lett. 13 (1990), 129–134
- 2 A. Smontara, J.C. Lasjaunias, C. Paulsen, A. Bilušić, Y. Calvayrac, Mat. Sci. Eng. 294-296 (2000), 706–710
- 3 T. Klein, C. Berger, D. Mayou, F. Cyrot-Lackmann, Phys. Rev. Lett. 66 (1991), 2907–2910
- 4 T. Klein, H. Rakoto, C. Berger, G. Fourcaudot, F. Cyrot-Lackmann, Phys. Rev. B 45 (1992), 2046–2049
- 5 P. Lindqvist, C. Berger, T. Klein, P. Lanco, F. Cyrot-Lackmann, Y. Calvayrac, Phys. Rev. B 48 (1993), 630–633
- 6 D. Mayou, C. Berger, F. Cyrot-Lackmann, T. Klein, P. Lanco, Phys. Rev. Lett. 70 (1993), 3915–3918
- 7 M. Ahlgren, P. Lindqvist, M. Rodmar, Ö. Rapp, Phys. Rev. B 55 (1997), 14847–14854
- 8 R. Escudero, J. C. Lasjaunias, Y. Calvayrac, M. Boudard, J. Phys.: Condens. Matter 11 (1999), 383–404
- 9 A. Bilušić, A. Smontara, J.C. Lasjaunias, J. Ivkov, Y. Calvayrac, Mat. Sci. Eng. 294-296 (2000), 711–714
- 10 A. Bilušić, I. Bešlić, J. Ivkov, J.C. Lasjaunias, A. Smontara, Fizika A (Zagreb) 8 (2000), 183–194
- 11 C.V. Landauro, H. Solbrig, Mat. Sci. Eng. A 294-296 (2000), 600–603
- 12 H. Solbrig, C.V. Landauro, Quasicrystals, Structure and Physical Properties, Wiley-VCH, Weinheim 2003, 254
- 13 A. Perrot, J.M. Dubois, M. Cassart, J.P. Issi, Proc. of the 5th Inter. Conf. on Quasicrystals, World Scientific, Singapore, 1995, 588–601
- 14 K. Fukamichi, Physical Properties of Quasicrystals, Springer, New York 1999, p. 295 and references therein
- 15 Y. Yokoyama, Y. Matsuo, K. Yamamoto, K. Hiraga, Mater. Trans., JIM, 43 (2002), 762–765
- 16 C. V. Landauro, H. Solbrig, Physica B 301 (2001), 267–275

- ¹⁷ N. W. Aschcroft, N. D. Mermin, *Solid State Physics*, Saunders College Publishing, London 1976, 46
- ¹⁸ F. S. Pierce, P. A. Bancel, B. D. Biggs, Q. Guo, S. J. Poon, *Phys. Rev. B* 47 (1993), 5670–5676
- ¹⁹ H. Solbrig, C. V. Landauro, A. Löser, *Mat. Sci. Eng. A* 294–296 (2000), 596–599
- ²⁰ J. Dolinšek, S. Vrtnik, M. Klanjšek, Z. Jagličić, A. Smontara, I. Smiljanić, A. Bilušić, Y. Yokoyama, A. Inoue, C.V. Landauro, *Phys. Rev. B* (in press)
- ²¹ D.-M. Zhu, *Phys. Rev. B* 50 (1994), 6053–6056
- ²² R. Mévrel, J.-C. Laizet, A. Azzopardi, B. Leclercq, M. Poulain, O. Lavigne, D. Demange, *J. Eur. Cer. Soc.* 24 (2004), 3081–3089
- ²³ Ž. Bihar, A. Bilušić, J. Lukatela, A. Smontara, P. Jeglič, P. J. McGuinness, J. Dolinšek, Z. Jagličić, J. Janovec, V. Demange, J. M. Dubois, *J. Alloys Compd.* 407 (2006), 65–73
- ²⁴ J. Dolinšek, P. Jeglič, P. J. McGuinness, Z. Jagličić, A. Bilušić, Ž. Bihar, A. Smontara, C.V. Landauro, M. Feuerbacher, B. Grushko, K. Urban, *Phys. Rev. B* 72 (2005), 064208–11
- ²⁵ A. Bilušić, A. Smontara, J. Dolinšek, P. J. McGuinness, H. R. Ott, *J. Alloys Compd.* 432 (2007), 1–6
- ²⁶ A. Smontara, I. Smiljanić, A. Bilušić, Z. Jagličić, M. Klanjšek, S. Roitsch, J. Dolinšek, M. Feuerbacher, *J. Alloys Compd.* 430 (2007) 29–38
- ²⁷ A. Smontara, I. Smiljanić, A. Bilušić, B. Grushko, S. Balanetskyy, Z. Jagličić, S. Vrtnik, J. Dolinšek, *J. Alloys Compd.*, in press
- ²⁸ J. Dolinšek, T. Apih, P. Jeglic, I. Smiljanic, A. Bilusic, Ž. Bihar, A. Smontara, Z. Jaglicic, M. Heggen, M. Feuerbacher, *Intermetallics* 15 (2007) 1367–1376
- ²⁹ A. Bilušić, Ž. Budrović, A. Smontara, J. Dolinšek, P. C. Canfield., I. R. Fisher, *J. Alloys Compd.* 342 (2002), 413–415
- ³⁰ R. Berman, *Thermal Conduction in solids*, Clarendon Press, Oxford 1978, 23
- ³¹ P. A. Kalugin, M. A. Chernikov, A. Bianchi, H. R. Ott, *Phys. Rev. B* 53 (1996), 14145–14151
- ³² J. C. Lassjaunias, Y. Calvayrac, H. Yang, *J. Physique* 17 (1997), 959–976
- ³³ Y. Amazit, M. de Boissieu, A. Zarembowitch, *Europhys. Lett.* 20 (1992), 703–706
- ³⁴ A. Bilušić, D. Pavuna, A. Smontara, *Vacuum* 61 (2001), 345–348